

Speckles generated from higher order optical vortices

Salla Gangi Reddy*,¹ Shashi Prabhakar,¹ Ashok Kumar,² J. Banerji,¹ and R. P. Singh¹

¹Physical Research Laboratory, Navarangpura, Ahmedabad, India - 380009

²Instituto de Fisica, Universidade de Sao Paulo, Sao Paulo, 66318, Brazil.

*sgreddy@prl.res.in

(Dated: October 27, 2022)

We have experimentally generated speckles from the optical vortices of different orders. It has been observed that the transverse size of generated speckles decreases with increase in the order of vortex passing through a static ground glass plate. We show experimentally as well as theoretically and numerically that the area of the bright ring of an optical vortex increases with its order. Thus, the decrease in speckle size can be attributed to the increase in area of illumination on the ground glass.

Optical vortices are phase singularities or screw dislocations in the light field [1]. These vortices have helical wavefront and the Poynting vector of such fields rotates around the propagation axis of the light. Due to such rotation of the Poynting vector, optical vortices carry an orbital angular momentum $m\hbar$ per photon, m is called the azimuthal index or topological charge of the vortex. The spatial structure of the optical vortices looks like a ring with a dark core at the center [2, 3]. Due to their peculiar properties, they have been getting a lot of attention and finding applications in optical manipulation as well as quantum information and computation [4, 5].

Speckles or granular pattern of intensity maxima and minima were first recognized by the reflection of a coherent light from a rough surface: such pattern originates due to the interference of many reflected waves having random phases [6]. This phenomenon can also occur in the scattering of the coherent light beam through a rough surface such as a ground glass [7]. The contrast of the speckle pattern formed by a coherent or monochromatic light source is maximum and it decreases with increase in the linewidth of the source [8]. The size of the speckle is directly proportional to the propagation distance and inversely proportional to the square root of area of illumination of the incident beam on the rough surface [9]. It also depends on the number of scatterers present in a given area of illumination i.e. grain size of the rough surface. At the same time, the transverse coherence length of the scattered light depends on the size of the speckle [10]. The speckles have a lot of significance in optical coherence tomography and usefulness in differentiating various types of tissues [11, 12]. These patterns play an important role in understanding the physics behind the thermal ghost imaging in which speckle-speckle correlation replaces photon correlations in quantum domain [13–16]. The resolution and contrast of the ghost imaging also depends on the size of the speckles [17–19].

It has been known that the speckles generated by a coherent light field also contain the phase singularities and their density in a given speckle pattern is directly proportional to the reciprocal of speckle size [20]. In the present study, we generate speckles from optical vortices with different orders. It is interesting to study the speckles generated from the phase singularities as speckles themselves consist of phase singularities. We use a static ground glass (SGG) plate to scatter the optical vortices of different orders and study the dependence of the generated speckle size on the order of vortex.

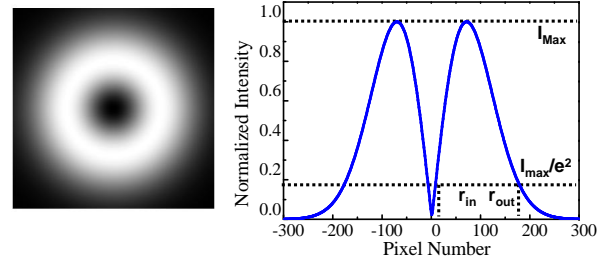


FIG. 1. The transverse intensity distribution of an optical vortex of order 1 and its line profile.

The intensity distribution of a vortex of order m , embedded in a Gaussian host beam of width w_0 is given by

$$I_m(r) = r^{2m} \exp\left(-\frac{2r^2}{w_0^2}\right), \quad r^2 = x^2 + y^2. \quad (1)$$

This intensity distribution is shown in Fig 1. Here, we are defining two parameters for a vortex beam: inner and outer radii (r_1, r_2). These are the radial distances at which the intensity falls to $1/e^2$ (13.6%) of the maximum intensity at $r = r_0$ (say). Here, r_1 is the point closer to the origin or the center and r_2 is the point farther from the center, the outer region of the beam. The distances r_i ($i = 0, 1, 2$) can be obtained as follows. For the sake of convenience, we set $w_0 = 1$, that is, w_0 is the unit of measuring radial distances. We also define $\chi = r^2$ and $\chi_i = r_i^2$ ($i = 0, 1, 2$) so that $I_m(r) = J_m(\chi) = \chi^m \exp(-2\chi)$. Differentiating $J_m(\chi)$ with respect to χ , one easily obtains $\chi_0 = m/2$ so that the maximum intensity has the value $J_m(\chi_0) = \chi_0^m \exp(-2\chi_0)$. The equations for χ_1 and χ_2 can then be written as

$$\chi_1^m \exp(-2\chi_1) = \chi_0^m \exp(-2\chi_0 - 2) \quad (2a)$$

$$\chi_2^m \exp(-2\chi_2) = \chi_0^m \exp(-2\chi_0 - 2). \quad (2b)$$

These equations have been solved numerically in *Mathematica* [21] for $m > 0$. The numerical values are tabulated in Table I and plotted in Fig. 2.

Remarkably, it is found that to a very good approximation,

$$\chi_2 + \chi_1 = m + 1.3. \quad (3)$$

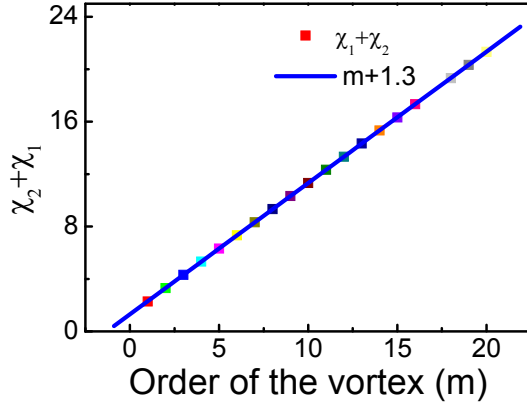


FIG. 2. Numerically obtained values of $\chi_2 + \chi_1$ (filled squares) and the line $y = m + 1.3$ as functions of m .

TABLE I. Numerical solutions for Eqs. (2a) and (2b)

m	χ_1	χ_2	$\chi_2 + \chi_1$	m	χ_1	χ_2	$\chi_2 + \chi_1$
1	0.0262	2.2526	2.2789	13	3.5280	10.8008	14.3288
2	0.1586	3.1462	3.3048	14	3.8931	11.4360	15.3291
3	0.3602	3.9538	4.3140	15	4.2630	12.0664	16.3294
4	0.6034	4.7154	5.3188	16	4.6370	12.6927	17.3296
5	0.8748	5.4469	6.3216	17	5.0148	13.3150	18.3299
6	1.1667	6.1569	7.3236	18	5.3962	13.9339	19.3301
7	1.4746	6.8504	8.3250	19	5.7807	14.5495	20.3302
8	1.7951	7.5309	9.3260	20	6.1682	15.1622	21.3304
9	2.1262	8.2006	10.3268
10	2.4662	8.8613	11.3274	50	18.5793	32.7529	51.3321
11	2.8138	9.5142	12.3280	100	40.6553	60.6775	101.3330
12	3.1680	10.1605	13.3284	200	86.5165	114.8165	201.3330

This empirical relationship can now be used to obtain simple expressions for χ_1 and χ_2 . Multiplying the left sides of Eqs (2a) and (2b), using Eq. 3 and the formula $(\chi_2 + \chi_1)^2 + (\chi_2 - \chi_1)^2 = 4\chi_1\chi_2$, we get

$$\chi_2 - \chi_1 = \sqrt{q_m}, \quad q_m = (m + 1.3)^2 - m^2 \exp(-1.4/m). \quad (4)$$

Solving Eqs. (3) and (4), we get χ_1, χ_2 and hence, r_1, r_2 :

$$r_1 = (m + 1.3 - \sqrt{q_m})^{1/2} / \sqrt{2} \quad (5a)$$

$$r_2 = (m + 1.3 + \sqrt{q_m})^{1/2} / \sqrt{2}. \quad (5b)$$

The area of the bright region in an optical vortex is given by

$$A_m = \pi(\chi_2 - \chi_1) = \pi \sqrt{q_m} \quad (6)$$

which clearly depends on the order (m) of the vortex (see Eq. 4).

We also show experimentally the dependence of the area of the bright region of optical vortices on their orders. Fig. 3

shows the line profiles of optical vortices for orders 0-6 produced in the laboratory using computer generated holography (CGH) technique. We have determined inner and outer radii of the vortex beams from the corresponding line profiles. The variation of inner and outer radii for vortex beams and the area of the bright region are shown in Fig. 4. In these plots, the experimental data is shown with solid lines and theoretical data (obtained from Eq. 5) with dotted lines. The experimental findings are in good agreement with the theoretical values.

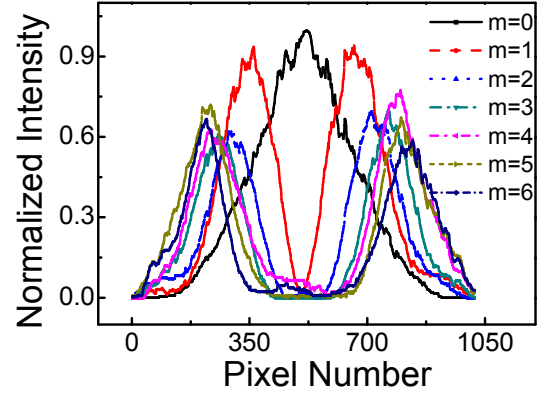


FIG. 3. Line profiles along the vortex centres of optical vortices for orders 0-6 which are produced in the laboratory

Next, we will discuss how the area of bright region is related to the speckle size. It is well known that the average size of the speckles generated by the scattering of a coherent (monochromatic) light beam through a rough object such as ground glass varies directly to the propagation distance and inversely to the area of incident light beam [22] for a given wavelength. From this, it is clear that the speckle size decreases with increase in the area of the incident beam. We have shown above that the area of the bright region in an optical vortex increases with its order. Therefore, one can infer that the speckle size decreases with the order of vortex.

Our experimental setup for the generation of speckles from optical vortices is shown in Fig. 5. An intensity stabilized He-Ne laser of power 1 mW and beam waist 0.3 mm is used to generate optical vortices. The optical vortex beams are produced by computer generated holography using a spatial light modulator (SLM). Different computer generated holograms for generating different vortices are introduced to the SLM through a computer. The required beam is selected with an aperture A_1 , and passed through the SGG plate. The scattered light from the SGG plate contains the granular pattern of intensity maxima and minima or speckles, as shown in Fig 6 (a). These speckles are recorded with a CCD camera. The SLM is placed at a distance of 60 cm from the laser and the SGG plate is at a distance of 66 cm from the SLM while the CCD camera is placed at 18 cm from the SGG plate.

The size of the recorded speckles has been determined by using auto-correlation method [8] which calculates the corre-

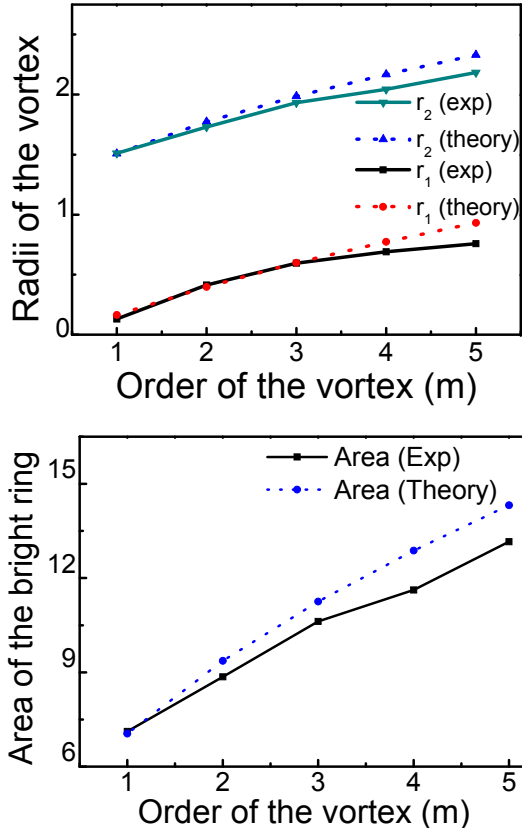


FIG. 4. Experimental (solid) and theoretical (dotted) results showing the variation of (a) inner and outer radii and (b) area of bright region with the order of a vortex.

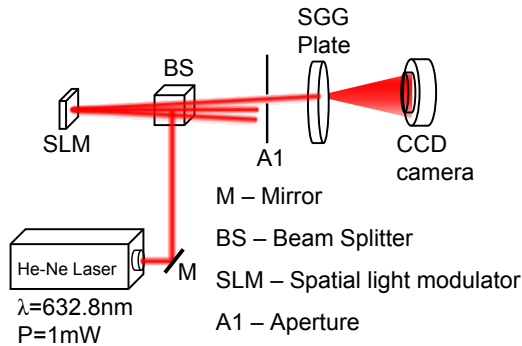


FIG. 5. The experimental set-up for the generation and recording of speckles from optical vortices.

lation of speckle field with itself. In this method, we fix one image of the speckles and observe its correlation with a number of images shifted in position. The shifts can be made pixel by pixel in both the transverse directions. We plot the results as a function of the shift. The correlation factor is maximum if two fields are completely overlapped and it decreases with the decrease in the overlap extent. The correlation factor becomes zero if their overlap extent is greater than the speckle

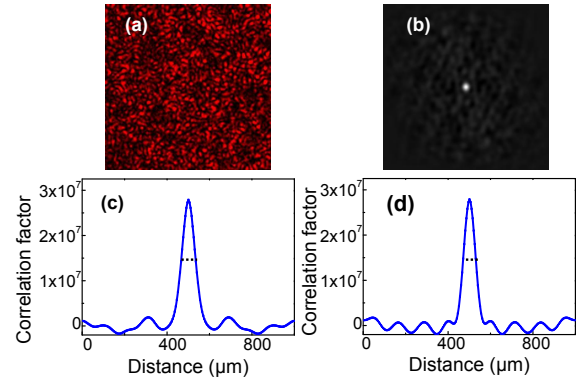


FIG. 6. (a) The obtained speckle pattern, (b) the distribution of auto correlation function, (c) and (d) are the variation of autocorrelation function in both transverse directions X and Y respectively.

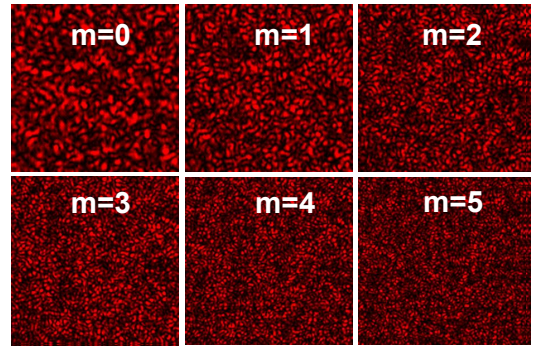


FIG. 7. The speckle patterns formed by the vortices with orders $m = 0 - 5$.

size due to the random nature of field. The correlation curve has a Gaussian distribution whose full width at half maximum (FWHM) gives the speckle size in any of the transverse directions.

Fig 6 (a) shows the speckle pattern formed by the scattering of first order vortex through a SGG plate. The size of the autocorrelation function (ACF) is always twice the considered size of the speckle pattern as we are observing correlation along both positive and negative directions. To find the size of recorded speckles, we have chosen 200×200 pixel sized speckle pattern and its autocorrelation as shown in Fig 6 (a) and 6 (b) respectively. The distributions of the autocorrelation function in two transverse directions have been shown in Figs 6 (c) and (d). The FWHM of these two distributions give the speckle size in the corresponding transverse directions.

Fig 7 shows the speckle patterns formed by the scattering of optical vortices of orders 0-5 through the same SGG plate. The speckle size S_m decreases with the increase in order m . The dependence of $\ln S_m$ on $\ln A_m$, (A_m , the area of the bright region of an optical vortex) is shown in Fig. 8. From the graph, it is clear that the speckle size decreases as the order of the vortex increases. The curve is a straight line with slope equal to the power of A_m on which speckle size depends. With

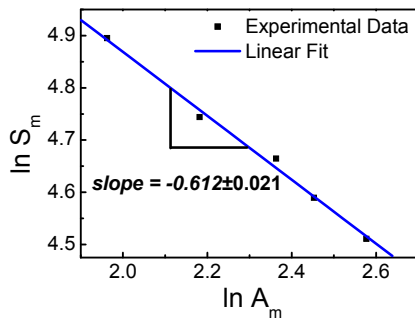


FIG. 8. The plot of $\ln S$ versus $\ln A_m$ where S and A_m are the experimentally obtained speckle size and area of bright region. The solid line is the best fit for our experimental data.

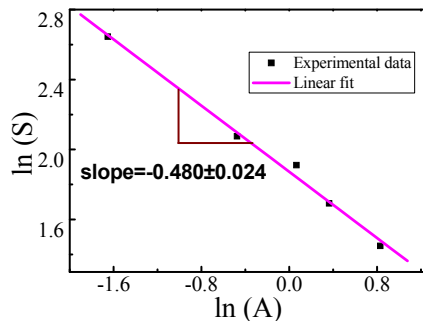


FIG. 9. The plot of $\ln S$ versus $\ln A$ where S and A are the experimentally obtained speckle size and area of a Gaussian beam. The solid line is the best fit for our experimental data.

the best fit to our experimental data, we have found that the speckle size is directly proportional to $A_m^{-0.612 \pm 0.021}$. The experimental data as well as the best fit curve to our experimental data have been shown in Fig. 8. It is different from the speckle size obtained with a Gaussian beam. For a Gaussian beam scattered through a ground glass plate, one expects a Brownian distribution of speckles and in fact gets speckle size proportional to $A^{-0.50}$ [22]. We have verified this experimentally and shown in Fig. 9. This suggests the non-Gaussian statistics of the speckles generated by the scattering of optical vortex beams.

It is known in the context of imaging that the spatial noise due to the speckles decreases if more number of speckles are present [7]. We have shown that the speckle size decreases with the order of the vortex which effectively increases the number of speckles present in a given area. Thus one can say that the spatial noise due to the speckles decreases with the order of vortex.

In conclusion, we have experimentally shown that the size of the speckle decreases with the order of the vortex. This decrease is attributed to the increase in the area of bright region of optical vortices. We have explained the structure of the vortex in a novel way and we have quantified the area of bright ring of vortex in terms of its order; which can also be utilized to determine the order of an unknown vortex. A study of speckles formed by the optical vortices may find applications in ghost imaging with vortices.

-
- [1] J. F. Nye and M. V. Berry, Proc. R. Soc. Lond. A Math. Phys. Sci. **336(1605)**, 165190 (1974).
 [2] J. E. Curtis, and D. G. Grier, Phys. Rev. Lett. **90**, 133901 (2003).
 [3] A. Kumar, P. Vaity, Y. Krishna, and R. P. Singh, Opt. Lasers Eng. **48**, 276 (2010).
 [4] L. Allen, S. M. Barnett, and M. J. Padgett, *Optical Angular Momentum* (IOP, 2003).
 [5] G. M. Terriza, J. P. Torres, and L. Torner, Nature Phys. **3**, 305–310 (2007).
 [6] J. D. Rigden, and E. I. Gordan, Proc. IRE, **50:2367**, (1962).
 [7] J. C. Dainty, *Laser Speckle and related phenomena* (Springer Verlag, 1984).
 [8] J. W. Goodman, *Speckle phenomena in optics*, (Indian edition 2008).
 [9] J. W. Goodman, J. Opt. Soc. Am., **66**, 1145 (1976).
 [10] T. Asakura, Opto Electronics **2**, 115 (1970).
 [11] B. Karamata, K. Hassler, M. Laubscher, and T. Lasser, J. Opt. Soc. Am. A, **22**, 593 (2005).
 [12] D. A. Zimnyakov, V. V. Tuchin, and A. A. Mishin, Appl. Opt., **36**, 5594 (1997).
 [13] A. Gatti, E. Brambilla, M. Bache, and L. A. Lugiato, Phys. Rev. Lett. **93**, 093602 (2004).
 [14] L. Basano, and P. Ottonello, Appl. Phys. Lett. **89**, 091109 (2006).
 [15] F. Ferri, D. Magatti, V. G. Sala, and A. gatti, Appl. Phys. Lett. **92**, 261109 (2008).
 [16] W. Gong, P. Zhang, X. Shen, and S. Han, Appl. Phys. Lett. **95**, 071110 (2009).
 [17] S. Crosby, S. Castelletto, C. Aruldoss, R. E. Scholten, and A. Roberts, New J. Of Phys. **9**, 285 (2007).
 [18] M. N. OSullivan, K. W. C. Chan, and R. W. Boyd, Phys. Rev. A **82**, 053803 (2010).
 [19] K. W. C. Chan, M. N. O’Sullivan, and R. W. Boyd, Opt. Exp. **18** 5562 (2010).
 [20] W. Wang, S. G. Hanson, Y. Miyamoto, and M. Takeda, Phys. Rev. Lett. **94**, 103902 (2005).
 [21] Details can be found at <http://www.wolfram.com>.
 [22] R. Sirohi, *Optical Methods of Measurements*, (Marcel Dekker, 1999).